Journal of Oil Palm Research Vol. 37 (3) September 2025 p. 519-532
DOI: https://doi.org/10.21894/jopr.2024.0042

SULPHONIC ACIDS SUPPORTED ON Fe_3O_4/PVA MAGNETIC COMPOSITE AS CATALYSTS FOR ESTERIFICATION OF FREE FATTY ACIDS

ANDREW T H YEOW[1,2]; ADEEB HAYYAN[1,2]*; MOHD USMAN MOHD JUNAIDI[1,2]; MUNEER M BA-ABBAD[3] and MOHD ALI HASHIM[1]

ABSTRACT

Low-quality palm oil (LPO) with high free fatty acid (FFA) content (9.66%) can be pretreated for biodiesel production through acid-catalysed esterification. However, homogeneous acid catalysts exhibit challenges in recyclability and separation despite their high catalytic efficiency. Magnetic composites (Fe_3O_4/PVA) as support materials for acid catalysts are a viable protocol for improving recyclability and separation performances. In this study, sulphonic acids and their deep eutectic solvent (DES) counterparts (formed with paracetamol at a 3:1 molar ratio) were supported on Fe_3O_4/PVA to yield heterogeneous solid acid catalysts for FFA esterification in LPO. From the screening results, Fe_3O_4/PVA/PTSA was determined as the best performing catalyst. The optimised reaction conditions were determined: 10 wt.% catalyst loading, 20:1 methanol-to-oil molar ratio, 5 hr of contact time and at 60°C, resulting in an FFA conversion of 79.81%. Fe_3O_4/PVA/PTSA exhibited fair recyclability performances and stability with >65% FFA conversion after five successive runs. FFA esterification reaction using Fe_3O_4/PVA/PTSA was determined to require an activation energy of 43.72 kJ/mol following a simplified pseudo first order rate of reaction. Pristine sulphonic acids exhibited higher compatibility to be supported on Fe_3O_4/PVA magnetic composite than their DES counterpart, with Fe_3O_4/PVA/PTSA being a viable catalyst for the pretreatment of low-quality oils through FFA esterification.

Keywords: deep eutectic solvents, esterification, free fatty acid, magnetic composite, sulphonic acid.

Received: 11 January 2024; **Accepted:** 13 June 2024; **Published online:** 4 September 2024.

INTRODUCTION

Fossil fuel depletion and increased carbon emissions have spurred the need for renewable and sustainable alternative energy resources. Among such alternatives, biofuels such as biodiesels have garnered significant development as the most promising replacement for non-renewable, petroleum-derived diesel (Ghorbani-Choghamarani *et al.*, 2022). In the conventional production of biodiesel, edible vegetable oils from high yielding oil crops such as palm and sunflower oil undergo a highly scalable alkali-catalysed transesterification reaction process to yield fatty acid methyl esters (FAME), a form of biodiesel and glycerol. The use of edible, refined vegetable oils in biodiesel production poses concerns over food supply competition and high production costs (Tropecêlo *et al.*, 2016). Recently, biodiesel production through the valorisation of low value, non-edible feedstocks such as sludge oils, waste vegetable oils or animal fats and used cooking oil has garnered significant attention (Maleki *et al.*, 2022; Yu *et al.*, 2021). Here, the feedstocks can undergo acid-catalysed esterification as a

[1] Department of Chemical Engineering, Faculty of Engineering, Universiti Malaya, 50603 Kuala Lumpur, Malaysia.

[2] Sustainable Process Engineering Centre (SPEC), Faculty of Engineering, Universiti Malaya, 50603 Kuala Lumpur, Malaysia.

[3] Gas Processing Center, College of Engineering, Qatar University, P.O. Box 2713 Doha, Qatar.

* *Corresponding author e-mail: adeeb.hayyan@yahoo.com*

pre-treatment step prior to the transesterification reaction to reduce the high free fatty acid (FFA) content. The utilisation of low value, non-edible feedstocks through catalytic esterification eliminates the aforementioned competition with food supply and improves the economic feasibility of biodiesel production (Bahadoran *et al.*, 2022; Chen *et al.*, 2023). Therefore, the development of acidic catalysts that are commercially significant is vital to enable effective valorisation of low value feedstocks to improve the economic feasibility of biodiesel production (Lou *et al.*, 2023).

Acidic catalysts in the esterification process for biodiesel production can be broadly classified into homogeneous- and heterogeneous-type catalysts. Mineral acids such as sulphuric acid are commonly employed as homogeneous catalysts, however, have significant drawbacks such as being highly corrosive, requiring complex downstream separation and exhibiting challenges in recyclability (Khan *et al.*, 2021). Recent advancements in homogeneous acidic catalysts such as ionic liquids and deep eutectic solvents (DESs) have been sought out due to their unique properties in overcoming the limitations of conventional mineral acids (Hayyan *et al.*, 2023; He *et al.*, 2023; Wang *et al.*, 2022). On the other hand, solid acid catalysts (SACs) have garnered significant development as a heterogeneous catalyst material for the biodiesel esterification process owing to its advantages over homogeneous catalysts, such as being recyclable, having lower corrosiveness and enabling sustainable catalyst design, particularly when derived from biomass (Zhou *et al.*, 2023). A relevant catalyst design protocol is through supporting homogeneous acids onto various types of support materials such as mesoporous silicas, layered double hydroxides, metal organic frameworks (MOFs), carbon-based materials and polymers (Borton *et al.*, 2019; Chen *et al.*, 2022; Mandari & Devarai, 2022; Zhong *et al.*, 2019). Furthermore, the catalyst recovery and recyclability of the SACs can be enhanced with the integration of a magnetic component such as ferromagnetic magnetite nanoparticles (Fe_3O_4), yielding magnetic responsive SACs that can be easily separated from the reaction mixture via magnetic forces introduced externally (Krishnan *et al.*, 2021). Hence, various magnetic composite/nanocomposite catalyst materials have been investigated for catalytic applications in biodiesel production (Xie & Li, 2023). For example, Ali *et al.* (2020) reported on the synthesis of cuprospinel ($CuFe_2O_4$)-based magnetic nanocatalyst for waste frying oil transesterification that exhibited exceptional biodiesel yield (90.24%) and ease of separation and recovery magnetically. 1-butyl-3-methylimidazolium hydrogen sulphate acidic ionic liquid was synthesised and supported on a Fe_3O_4/SiO_2 composite for the methyl esterification reaction of waste seed oils (Yu *et al.*, 2021). The authors reported high catalytic efficiency and stability (87.6% conversion after four reaction cycles) while exhibiting ease of separation due to its magnetic properties.

In a previous study, sulphonic acids in the form of DESs were reported for the esterification of mixed oils with high FFA content (Hayyan *et al.*, 2023). Herein, p-toluenesulphonic acid was combined with paracetamol to form a DES (3:1 molar ratio) acting as a recyclable, homogeneous catalysts for FFA esterification. Despite the appreciable catalytic activity, the DES and its pristine acid counterparts exhibited weak recyclability. Therefore, the potential of the acids as heterogeneous catalysts in esterification reactions remains unexplored. This study investigates the feasibility of supporting sulphonic acids (BZSA, PTSA and SSA) and their DESs onto a Fe_3O_4/polyvinyl alcohol (PVA) magnetic composite material to improve its recyclability performance of the SACs for the esterification of FFA in LPO. PVA is a synthetic biopolymer that is widely used in fields of research materials such as PVA-based hydrogels for biomedical applications, functional materials and composites and as catalyst support materials due to its high thermal stability and good chemical resistance (Zhang *et al.*, 2016). PVA has been demonstrated as a viable composite/nanocomposite material with Fe_3O_4 magnetic nanoparticles (Maleki *et al.*, 2019; Rahimi *et al.*, 2020b). Additionally, the use of a crosslinker for the linking of PVA strands may enable better incorporation of the sulphonic acid functional group in the SAC (Perez & Dumont, 2021).

EXPERIMENTAL METHODS

Materials and Chemicals

Low-quality palm oil (LPO) containing high FFA content of 9.66% was supplied by a palm oil mill in Selangor, Malaysia. Anhydrous iron (III) chloride ($FeCl_3$, ≥98.00%) was obtained from HmbG Chemicals Malaysia, and iron (II) sulphate heptahydrate ($FeSO_4 \cdot 7H_2O$,≥99.50%) was obtained from R&M Chemicals Malaysia. Polyvinyl alcohol (PVA, molecular weight ~60,000, ≥98.00% degree of hydrolysis) and maleic acid (≥99.00%, Analytical reagent) were purchased from Merck Malaysia. The sulphonic acids involved in this study were: benzenesulphonic acid (BZSA, 90.00% technical grade, Sigma Aldrich), p-toluenesulphonic acid (PTSA, ≥98.00%, Sigma Aldrich), and 5-sulphosalicylic acid dihydrate (SSA, >99.00%, Merck). The sulphonic acids were used as supplied without further purification. Paracetamol (PCM, ≥99.00%, BioXtra grade) was obtained from Sigma Aldrich. Ammonium hydroxide solution ($NH_3.H_2O$, 25.00% w/v solution) was purchased

from R&M Chemicals Malaysia. Methanol (≥99.85%) and propan-2-ol (ACS reagent) were purchased from Kollin Chemicals and Merck Malaysia respectively.

Synthesis of Fe_3O_4/PVA Magnetic Composite

Fe_3O_4/PVA magnetic composites were synthesised based on the *in-situ* co-precipitation method (Fazelinia *et al.*, 2023; Kamalzare *et al.*, 2021). A 5 w/v % PVA solution was produced by dissolving PVA in distilled water under vigorous stirring for 4 hr at 80°C. Subsequently, 12 mL of $NH_3.H_2O$ was added to the PVA solution to adjust the pH to 11. At the same time, 0.02 mol of $FeCl_3$ and 0.01 mol of $FeSO_4.7H_2O$ were dissolved in 10 mL of distilled water to form a 2:1 Fe^{3+}:Fe^{2+} ratio mixture, serving as the Fe^{3+} and Fe^{2+} precursors for the synthesis of Fe_3O_4 magnetic nanoparticles by co-precipitation. This mixture was added dropwise into the $NH_3.H_2O$–PVA solution under stirring at 350 rpm. The solution gradually turned black and was continuously stirred for 2 hr at 60°C under N_2 atmosphere. The black particles precipitate (denoted as Fe_3O_4/PVA) was recovered using an external magnet and washed several times with distilled water and dried at 60°C overnight.

Synthesis of Sulphonic Acid-based DESs

To synthesise the sulphonic acid-based DESs, the sulphonic acids (BZSA, PTSA or SSA) were combined with PCM at a molar ratio of 3:1 (Hayyan *et al.*, 2023). The DESs are thus labelled as [3BZSA:PCM], [3PTSA:PCM] and [3SSA:PCM], corresponding to the sulphonic acid component and PCM. The DESs were formed under magnetic stirring (350 rpm) at 80°C for 1-3 hr until a homogeneous solution was obtained. The DESs were then collected and stored in a desiccator. After 24 hr of storage, the DESs remained in liquid phases at elevated temperature (60°C) and no precipitation was observed.

Synthesis of Acids and DESs Supported on Fe_3O_4/PVA

The synthesis protocol was adapted from the proposed method described by Kamalzare *et al.* (2021) with slight modifications. To synthesise the acid-supported Fe_3O_4/PVA, a 1:1 by mass ratio of Fe_3O_4/PVA and acid/DES was taken (Swami *et al.*, 2023). A total of 1 g of Fe_3O_4/PVA was dispersed in 15 mL of distilled water, and simultaneously 1 g of acid (BZSA, PTSA or SSA) or DES compound [3BZSA:PCM], [3PTSA:PCM], [3SSA:PCM] was dissolved in 10 mL of distilled water. The acid solution was added to the Fe_3O_4/PVA solution and continuously stirred for 15 min at ambient temperature. Subsequently, 30 wt.% of maleic acid was added as the crosslinker for the composite according to a previous optimisation study (Mok *et al.*, 2020) and 1 mL of 37% HCl was added to catalyse the crosslinking process. Finally, the mixture of synthesised composite (denoted as Fe_3O_4/PVA/Acid) was stirred for 30 min at room temperature, and subsequently collected using an external magnet. To remove any residuals remaining with composite, the Fe_3O_4/PVA/Acid was washed several times using distilled water and dried at 60°C overnight.

Esterification Reaction Experimental Setup

LPO was preheated to 70°C to yield a red, liquid phase oil that is homogeneous compared to its semisolid physical state at room temperature. The Fe_3O_4/PVA/Acid catalyst was added to the reactants of 20 g of LPO and methanol in a sealed, jacketed reactor equipped with an overhead condenser, where the mixture was stirred at 350 rpm constantly throughout the experiment. A screening stage was conducted to preliminarily evaluate the catalytic performance of the FFA esterification reaction and determine the most suitable catalyst including either the sulphonic acids or DES compounds supported on the Fe_3O_4/PVA magnetic composite. Subsequently, the preferred catalyst material was determined from the screening procedure for further characterisation and optimisation (by single factor optimisation). The optimisation parameters include catalyst loading within the range of 5-20 wt.%, methanol requirement within 10:1-25:1 methanol-to-oil molar ratio, contact time within 1-6 hr, and reaction temperatures 30°C-70°C. The esterification experiments were triplicated and the average FFA content is presented along with the standard deviation.

The FFA content was determined according to the American Oil Chemists Society (AOCS) Official Method Ca 5a-40 using titrimetric method (AOCS, 2017). The FFA limit was set for below 2%, and percentage conversion of FFA into FAME was determined according to Equation (1):

$$Conversion = \frac{FFA_I - FFA_F}{FFA_I} \times 100\% \quad (1)$$

where FFA_I and FFA_F are the initial and final FFA values before and after esterification respectively. The recyclability performance of the heterogeneous magnetic catalyst was also conducted. At the end of reaction, the catalyst was easily recovered using an external magnet and regenerated by washing repeatedly up to three times with distilled water and subjected to oven drying at 60°C overnight. The recovered catalyst was added to fresh LPO and the extent of the esterification reaction was evaluated.

Characterisation of Fe_3O_4/PVA/Acid Magnetic Composite

The synthesised Fe_3O_4/PVA/Acid was characterised for its morphology and elemental composition using field emission scanning electron microscopy (FESEM) imaging and energy dispersive X-ray spectroscopy (EDX) analysis (FEI Quanta FEG 650 S scanning electron microscope). The structural phase of the synthesised Fe_3O_4/PVA and Fe_3O_4/PVA/Acid were revealed using X-ray diffraction (XRD) analysis, which was conducted on the Malvern PANalytical EMPYREAN diffractometer system using CuKα radiation (λ = 1.5406 Å) at two theta (2θ) angle range of 10-80 (0.01 step size), and operated at 45 kV volts and 40 mA current. The thermogravimetric analyses (TGA) were conducted using a PerkinElmer Pyris 6 TGA analyser and the thermal behaviour was observed from 30°C-800°C at a 10°C/min heating rate under nitrogen gas flow. The energy binding and oxidation states of the Fe_3O_4/PVA/Acid composite were determined through X-ray photoelectron spectroscopy (XPS) conducted on the Axis Ultra DLD (KRATOS model) X-ray photoelectron spectrometer using a monochromated Al Kα radiation (1486.6 eV) as the excitation source (15 kV).

RESULTS AND DISCUSSION

Screening of Catalyst Performance in FFA Esterification

The screening of the catalyst performance was conducted at excess operating conditions (10 wt.% catalyst loading, 20:1 methanol-to-oil molar ratio, 6 hr contact time and reaction temperature at 60°C) to enable the reaction to achieve equilibrium. From the screening results presented in *Figure 1*, PTSA supported on Fe_3O_4/PVA (denoted as Fe_3O_4/PVA/PTSA) exhibited the highest catalytic performance, reducing the FFA value down to 1.98% below the predetermined limit, equivalent to 79.53% conversion; followed by Fe_3O_4/PVA/SSA at 66.51% FFA conversion. Among the list of catalysts supported on Fe_3O_4/PVA, the pristine acid components exhibited greater FFA conversion than their counterpart composed within the DES system. A plausible explanation for this may be that the DES system exhibited stronger molecular bonding with the water solvent while it was solvated, leading to the formation of an aqueous DES system (Picciolini *et al.*, 2023; Wang *et al.*, 2021). Hence, the DESs may be inferred to be incompatible with the Fe_3O_4/PVA composite based on the low FFA conversion results as the support was unable to exhibit a catalytic effect. BZSA and [3SSA:PCM] DES exhibited the weakest FFA esterification performance at 31.29% and 29.70% FFA conversion when supported on Fe_3O_4/PVA, which may be attributed to the weak attachment of the molecules and functional groups to the Fe_3O_4/PVA support material. Hence, Fe_3O_4/PVA/PTSA was determined as the best performing catalyst from the screening stage and further optimisation studies were conducted.

Characterisation of Fe_3O_4/PVA/PTSA

FESEM imaging and EDX analysis were used to provide topographical and elemental information of the synthesised Fe_3O_4/PVA/PTSA composite as presented in *Figure 2*, accompanied with the photographic images of the magnetic response of the Fe_3O_4/PVA/PTSA composite in water. The spherical shape of the Fe_3O_4/PVA/PTSA composite (*Figure 2a-2c*) observed from the FESEM image agrees with previously reported studies on modified Fe_3O_4/PVA (Maleki *et al.*, 2019). Furthermore, the elemental distribution of C (23.21%), Fe (46.11%), O (27.83%) and S (2.85%)

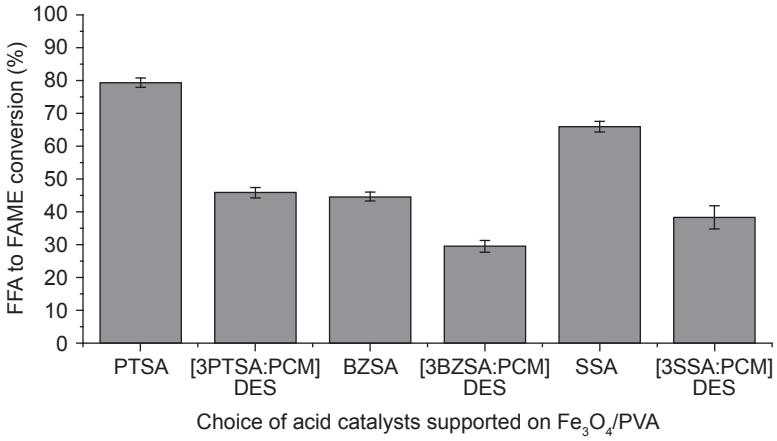

Figure 1. Screening of FFA esterification catalytic performance using sulphonic acids and DESs supported on Fe_3O_4/PVA magnetic composite.

was determined from the EDX analysis, suggesting that the PTSA is synthesised onto the Fe_3O_4/PVA matrix. The presence of the S element is contributed by the sulphonic acid functional group (-SO_3H) of the PTSA molecule, whereas the Fe and O element peaks in the EDX spectra plot affirm the presence of Fe_3O_4 (Ba-Abbad *et al.*, 2022). Additionally, the high carbon (C) element is attributed to the maleic acid-crosslinked PVA polymer chains and the benzene ring of the PTSA molecules. In summary, the EDX spectra plot elucidates the presence of Fe_3O_4, PVA and PTSA, thus supporting the screening results on the presence of catalytic activity for FFA esterification.

The TGA and derivative thermogravimetry (DTG) curves of the Fe_3O_4/PVA and Fe_3O_4/PVA/PTSA composite are presented in *Figure 3a* and *3b*. According to the DTG curves derived from the TGA data, two peaks were observed at 246.2°C-246.8°C and 441.4°C-460.2°C, which correspond to the breaking down of the polymer network of PVA and the dehydration of -OH groups among the PVA chains respectively (Kurchania *et al.*, 2014). Furthermore, the calculated peak at 86.17°C observed for the Fe_3O_4/PVA/PTSA curve may be attributed to the release of physically adsorbed water molecules arising from the acid modification step conducted extensively in the distilled water medium. The trends of the TGA curves were in good agreement with previously reported results in literature pertaining to the synthesis of Fe_3O_4/PVA (Maleki *et al.*, 2019).

The XRD pattern of the synthesised Fe_3O_4/PVA and Fe_3O_4/PVA/PTSA is presented in *Figure 3c*. The peaks appearing at 2θ = 30.15°, 35.54°, 43.33°, 53.58°, 57.32° and 62.78° are in good correlation with the standard JCPDS Card No. 88-0315 for Fe_3O_4 and affirms the synthesis. Furthermore, the broad peak centred at around 22° is assigned to the diffraction pattern of amorphous PVA (Maleki *et al.*, 2019). The XRD pattern for Fe_3O_4/PVA/PTSA revealed a fringe peak at 2θ = 32.69°, which may be attributed to the coating interaction between the PVA chains and the Fe_3O_4 particle (Rahimi *et al.*, 2020a, 2020b).

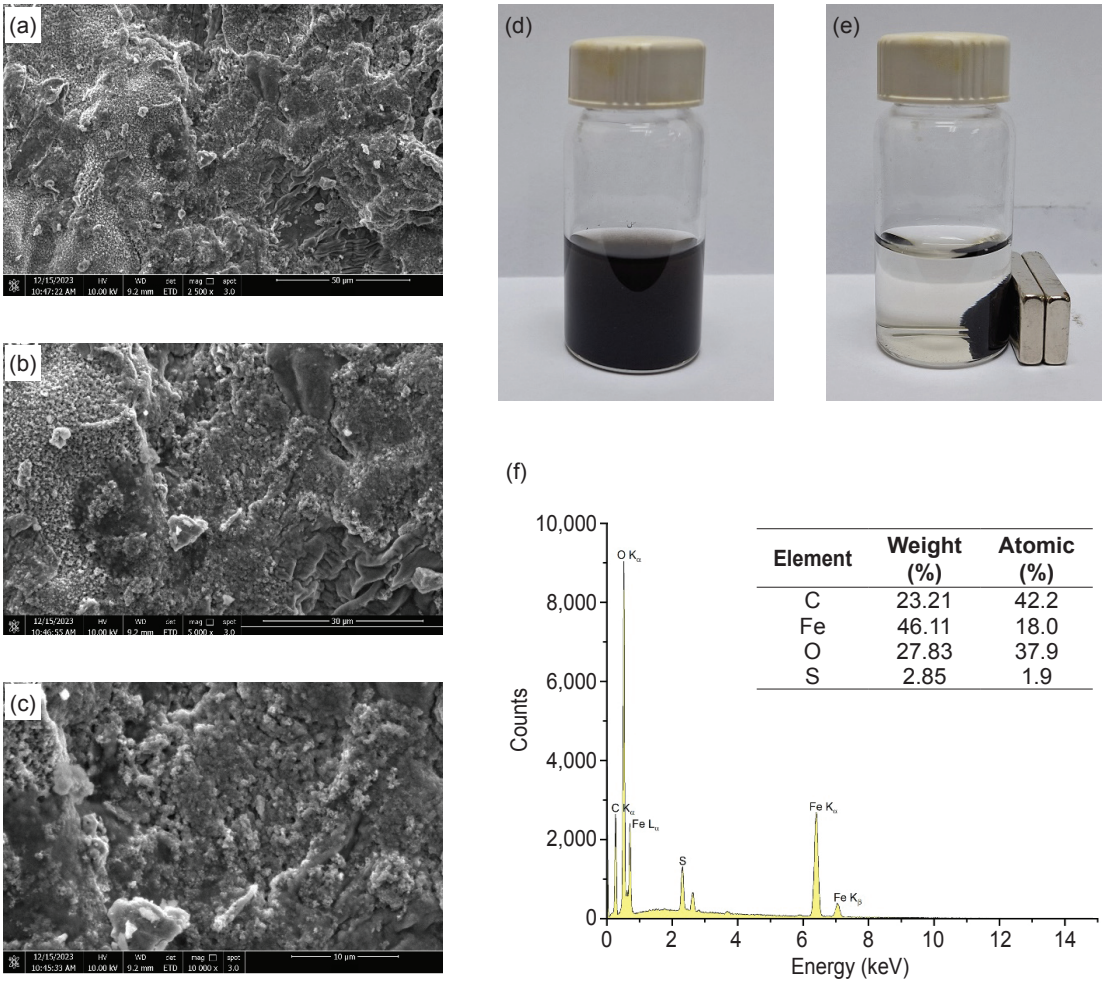

Figure 2. FESEM imaging of the Fe_3O_4/PVA/PTSA composite at (a) 2,500X, (b) 5,000X, and (c) 10,000X magnification; photographic image of (d) dispersion of Fe_3O_4/PVA/PTSA composite in water and (e) magnetic response of the Fe_3O_4/PVA/PTSA composite; and (f) EDX spectra plot of the Fe_3O_4/PVA/PTSA composite.

XPS spectra analysis was conducted to observe the near surface region of the Fe_3O_4/PVA/PTSA composite and determine the chemical states. *Figure 3d* presents the survey spectra of the Fe_3O_4/PVA/PTSA composite, indicating the detection of S 2p, O 1s, Fe 2p and C1s. The high resolution spectra of S 2p (*Figure 3e*) can be deconvoluted into two peaks at 168.3 and 169.6 eV that is assigned to the $-SO_3H$ groups of the PTSA molecule synthesised onto the surface of Fe_3O_4/PVA (Wang *et al.*, 2015; Zheng *et al.*, 2024). The three peaks determined in the deconvoluted O 1s spectra (*Figure 3f*) at 529.9, 531.2 and 532.4 eV may be assigned to oxygen in the form of Fe–O, H–O, and C–O respectively (Luo *et al.*, 2019). In the Fe 2p spectrum (*Figure 3g* and *3h*), the detection of asymmetric peaks at 710.5 and 724.1 eV (corresponding to the Fe $2p_{3/2}$ and Fe $2p_{1/2}$ phase) and the absence of a satellite peak at 719.0 eV verified the synthesis of Fe_3O_4-based composites (Ali *et al.*, 2018). The C 1s spectra were deconvoluted into three peaks at binding energies of 284.8, 286.3 and 288.6 eV that could be assigned to the functional groups of C–C, C–O and C=O respectively (Luo *et al.*, 2019). The XPS spectra did not reveal other peaks contributed by magnetic compounds such as FeO, FeOOH or Fe_2O_3. In summary, the XPS analysis confirms the successful synthesis of Fe_3O_4/PVA/PTSA composite, supported by the analytical results of XRD and TGA analysis.

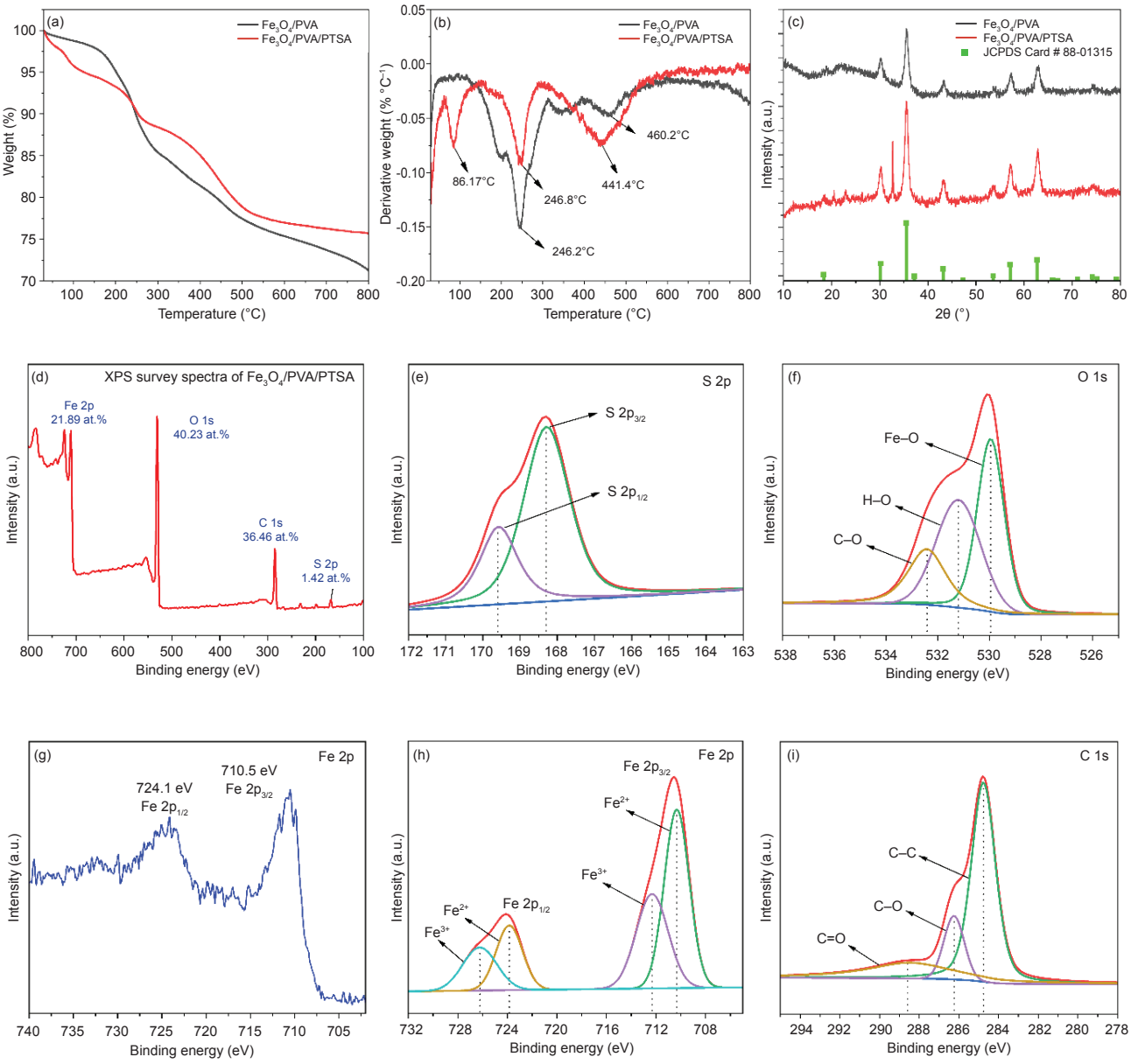

Figure 3. (a) TGA and (b) DTG curves of the Fe_3O_4/PVA and Fe_3O_4/PVA/PTSA composite; (c) XRD patterns for Fe_3O_4/PVA and Fe_3O_4/PVA/PTSA composite; (d) XPS survey spectrum and high-resolution XPS scan spectra over (e) S 2p, (f) O 1s, (g–h) Fe 2p and (i) C 1s for the Fe_3O_4/PVA/PTSA composite.

Effect of Catalyst Loading

The optimisation of Fe_3O_4/PVA/PTSA catalyst loading up to 20 wt.% on FFA esterification is presented in *Figure 4*. At 10 wt.% catalyst loading, the FFA value below 2.00% limit was achieved, equating to an FFA to FAME conversion percentage of 79.33%. At double catalyst loading as 20 wt.%, the FFA conversion rate of 84.38% was achieved. By increasing of catalyst loading, the FFA conversion rate was increased due to the increase of contact and density of the active sites to accelerate the reaction. Additionally, Wang *et al.* (2019) reported that novel synthesis of a magnetic sulphonated SAC based on zirconium and iron chelated using sodium alginate or sodium carboxymethylcellulose. The loading of the magnetic catalyst was studied from 3-11 wt.%, where 9 wt.% of catalyst loading achieved the highest biodiesel yield of 94.30% from the esterification of oleic acid. In another study, PTSA and methanesulphonic acid supported on UiO-66 MOFs were studied for the esterification of palmitic acids with methanol, n-butanol and n-decanol at 25 g/mol (10 wt.% of palmitic acid) of catalyst content (Liu *et al.*, 2020). Hence, the catalyst loading of 10 wt.% was reported in this study as optimum loading for the highest FFA conversion.

Effect of Methanol Requirement

Methanol is supplied as a reactant in excess by molar ratio to enable the forward shift of the FFA esterification reaction to yield FAME. The effects of the methanol ratio requirement on the FFA conversion rate are presented in *Figure 5*. At excess methanol: LPO molar ratio of 20:1, the final FFA content of 1.97% was attained, corresponding to a 79.61% FFA to FAME conversion. Increasing the methanol content to a 25:1 molar ratio resulted in a slight increase in the FFA conversion rate up to 81.07%. Considering the economic significance of excessive methanol with respect to the minute FFA conversion percentage, the optimum methanol: LPO molar ratio was selected as 20:1. In comparison, the methanol molar ratio requirement in the use of PTSA as a homogeneous catalyst is halved at 10:1 (Hayyan *et al.*, 2010). However, the excess methanol requirement is in good agreement with previous studies that used heterogeneous catalysts. Ibrahim *et al.* (2020) utilised oil palm empty fruit bunches to synthesise novel magnetic carbonaceous SAC for the esterification of palm fatty acid distillate. The magnetic catalyst enabled 96.00% conversion of the palm fatty acid distillate feedstock at the optimised methanol requirement of 16:1 molar ratio. Rokhum *et al.* (2022) reported on the influence and optimisation of a novel sugar-derived sulphonated aromatic carbon catalysts on oleic acid esterification, achieving 97.5% conversion at the optimised conditions of 20:1 methanol molar ratio and 5 wt.% catalyst loading.

Effect of Contact Time

Compared to homogeneous mineral acid catalysts applied in biodiesel esterification reactions, heterogeneous catalysts typically require extended contact time (Racar *et al.*, 2023). Hence, the catalyst contact time should be optimised to reach reaction equilibrium due to the increased mass transfer resistance and reduced surface area. The optimisation of catalyst contact time is presented in *Figure 6*. The FFA content was reduced down to 2.00% at the 5th hr of the reaction, and a slight reduction improvement in FFA content was recorded at 1.84% at the 6th hr. Durations of optimal catalyst contact time from 3-8 hr were reported in literature utilising various forms of heterogeneous catalysts. Sulphonated carbon catalysts derived from *Sargassum horneri* biomass were optimised for a high oleic acid conversion of 96.4% at a reaction time of 3 hr (Cao *et al.*, 2021). As reported, Xie and Wang (2020) synthesised polymeric 1-vinyl-3-(3-sulphopropyl)imidazolium hydrogen sulphate as acidic ionic liquids supported on Fe_3O_4/SiO_2 magnetic composites which yielded high oil conversion at 93.30% under optimal reaction time of 6 hr. Sulphonated ZnO-β-zeolite catalysts were reported to exhibit high catalytic performance (96.90% WCO conversion) in the simultaneous esterification and transesterification of waste cooking oil under optimal reaction time of 8 hr (Yusuf *et al.*, 2023).

Effect of Reaction Temperature

Higher reaction temperatures are required for FFA esterification reactions catalysed by heterogeneous catalysts (Maleki *et al.*, 2022). The influence of reaction temperature on the reduction of FFA content is presented in *Figure 7* and shows that the FFA conversion increased with increasing temperature from 40°C-70°C. At 60°C, the FFA was reduced to 1.96%, with no significant reduction observed for 70°C reaction temperature, indicating that the reaction equilibrium has been reached. Comparatively, phosphomolybdic acid was impregnated onto bismuth-based MOFs to yield SACs for the esterification of oleic acid (Zhang *et al.*, 2023). The esterification reaction was conducted in a sealed high-pressure autoclave that allowed reaction temperatures to be optimised between 120°C-170°C. As the reaction was conducted at atmospheric pressure in this study, the reaction temperature was optimised around the boiling point of methanol. Similarly,

the optimal reaction temperature was reported as 75°C in the transesterification of waste cooking oil in a glass batch reactor using a novel sulphonated Fe-Al-TiO_2 magnetic nanocomposite (Gardy *et al.*, 2018).

Validation of Reaction Conditions and Catalyst Recyclability

The reaction conditions determined in the optimum experiment conditions were: 10 wt.% acid catalyst loading, 20:1 methanol: LPO molar ratio of methanol loading, and 5 hr contact time at 60°C. The reaction conditions were revalidated and yielded a treated LPO sample with an FFA content value of 1.95% (79.81% FFA conversion). Subsequently, the catalyst recyclability study was conducted to evaluate the reusability of the Fe_3O_4/PVA/PTSA SAC. Upon completion of the first reaction run, the catalyst was easily recovered using an external magnet, washed continually several times using distilled water, and dried in a vacuum oven for 24 hr. Subsequently, the Fe_3O_4/PVA/PTSA catalyst was transferred to a fresh batch of LPO for the second used and succeeding reaction runs. The catalyst recyclability performance for five continuous reaction cycles is presented in *Figure 8*. The Fe_3O_4/PVA/PTSA catalyst maintained a relatively high FFA conversion rate in the first three runs, demonstrating a slight gradual decrease in FFA conversion from 79.81% to 78.89%. In the succeeding fourth and fifth reaction runs, the FFA conversion drops to 75.15% and 65.65% respectively. The decrease in

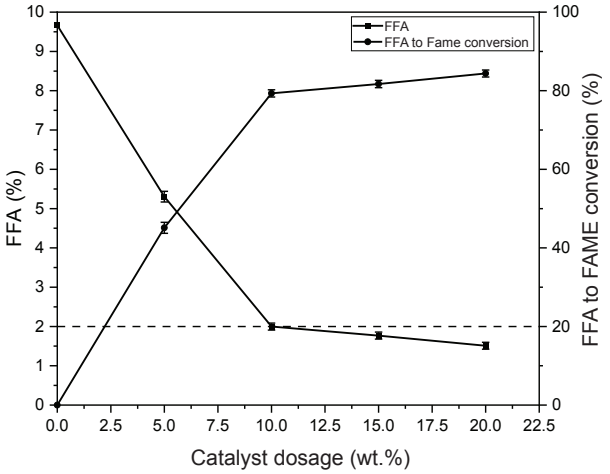

Figure 4. Effect of Fe_3O_4/PVA/PTSA catalyst loading on FFA content reduction and conversion. Experimental parameters were fixed at 20:1 methanol-to-oil molar ratio, 6 hr contact time and 60°C reaction temperature.

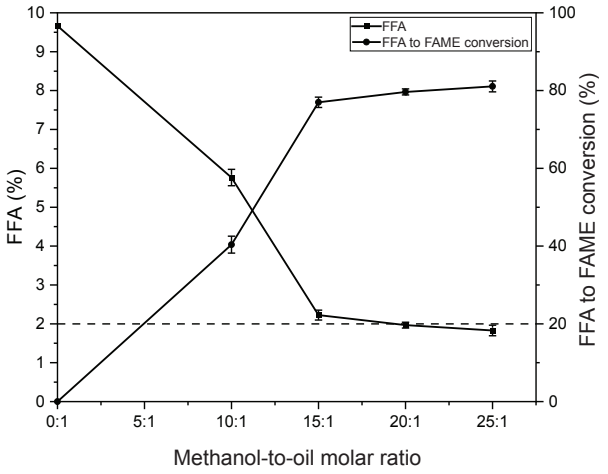

Figure 5. Effect of methanol requirement on FFA content reduction and conversion. Experimental parameters were fixed at 10 wt.% catalyst loading, 6 hr contact time and 60°C reaction temperature.

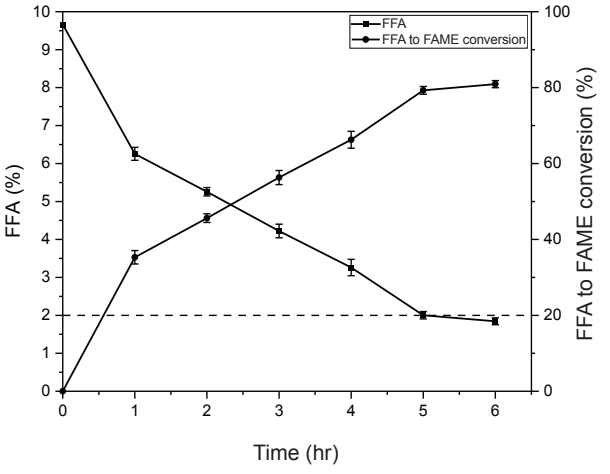

Figure 6. Effect of Fe_3O_4/PVA/PTSA catalyst contact time on FFA content reduction and conversion. Experimental parameters were fixed at 10 wt.% catalyst loading, 20:1 methanol-to-oil molar ratio and 60°C reaction temperature.

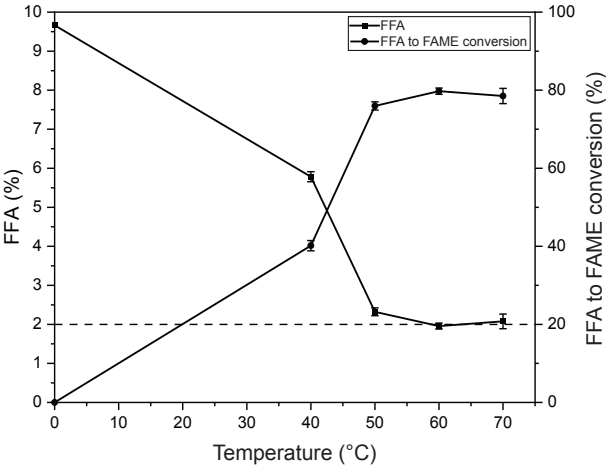

Figure 7. Effect of reaction temperature on FFA content reduction and conversion. Experimental parameters were fixed at 10 wt.% catalyst loading, 20:1 methanol-to-oil molar ratio and 5 hr contact time.

FFA conversion rate may be attributed to catalytic deactivation by water, by-product formation from the esterification reaction. To overcome this issue, the catalyst may be regenerated by re-sulphonation using PTSA (Cao *et al.*, 2021).

Evaluation of Reaction Kinetics and Thermodynamic Studies

The reaction kinetics and thermodynamic studies were presented for the FFA esterification reaction using Fe_3O_4/PVA/PTSA at the optimum reaction conditions at reaction temperatures of 40°C, 50°C and 60°C. Given that significant excess of methanol (20:1 molar ratio to oil) was used, and assuming the methanol concentration remained constant, the empirical data was fitted according to the pseudo first order kinetics based on a simple rate expression of the kinetic model (Hayyan *et al.*, 2023; Wang *et al.*, 2023). By plotting the rate constant (k) values against temperature, the activation energy (E_a) and frequency factor (A) were determined through the linearised form of the Arrhenius equation [Equation (2)].

$$k = Ae^{\frac{-E_a}{RT}} \tag{2}$$

Figure 9a depicts the Arrhenius plot with satisfactory coefficients of determination values ($R^2 > 0.9$) obtained. Here, the reaction kinetic factors of E_a and A values were calculated as 43.72 kJ/mol and 3.586/min respectively. The E_a values were in agreement with literature values on the esterification of low value oils using heterogeneous SACs between the range of 18.11-64.60 kJ/mol (Olagbende *et al.*, 2021; Zhang *et al.*, 2021).

Subsequently, the thermodynamic factors of the esterification reaction were studied through the Eyring-Polanyi model [Equation (3)]. The linearised plot of the Eyring-Polanyi model is expressed as Equation (4).

$$k = K\frac{k_B T}{h}e^{\left(\frac{\Delta G^\circ}{RT}\right)} \tag{3}$$

$$ln\left(\frac{k}{T}\right) = -\frac{\Delta H^\circ}{RT} + ln\left(\frac{k_B}{h}\right) + \frac{\Delta S^\circ}{R} + lnK \tag{4}$$

where, ΔH° is the standard enthalpy of the reaction system, ΔS° is the entropy of activation of the reaction system, k is the rate constant at temperature T, k_B is the Boltzmann constant, h is the Planck constant, K is the transmission coefficient ($K=1$), and R is the universal gas constant taken as 8.314 J/mol/K. The Gibbs free energy (ΔG°) was determined by Equation (5).

$$\Delta G^\circ = \Delta H^\circ - T\Delta S^\circ \tag{5}$$

The Eyring-Polanyi plot is illustrated in *Figure 9b*, showing satisfactory fitting based on the coefficients of determination values (R^2>0.9), and the thermodynamic parameters are presented in *Table 1*. Based on the results, the FFA esterification reaction using Fe_3O_4/PVA/PTSA was calculated as positive ΔH°, negative ΔS° and positive ΔG° values, which corresponds to the thermodynamics of the reaction process being dictated as endothermic, non-spontaneous and endergonic across the analysed temperature, respectively. The positive enthalpy values (ΔH°>0) dictate the requirement of external heat input for main product generation (FAME yield), attributed to the optimal reaction temperatures in FFA esterification. The results of this study were within range and in agreement with the thermodynamic parameters of SACs previously reported on the acid-catalysed esterification of FFA (Lieu *et al.*, 2016; Roslan *et al.*, 2022; Tang *et al.*, 2020).

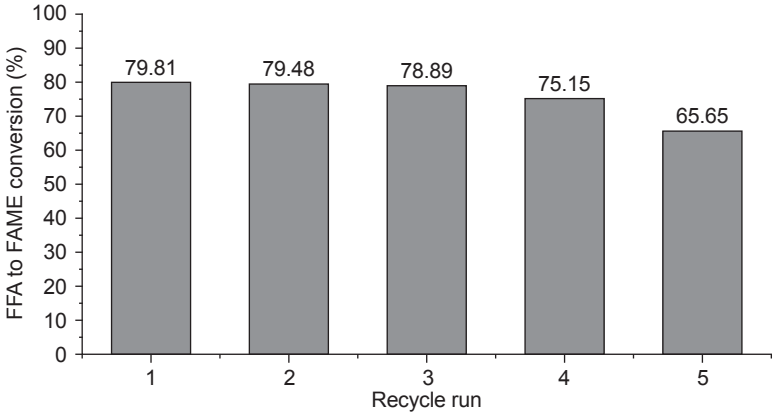

Figure 8. Evaluation of recyclability performance of Fe_3O_4/PVA/PTSA in FFA conversion.

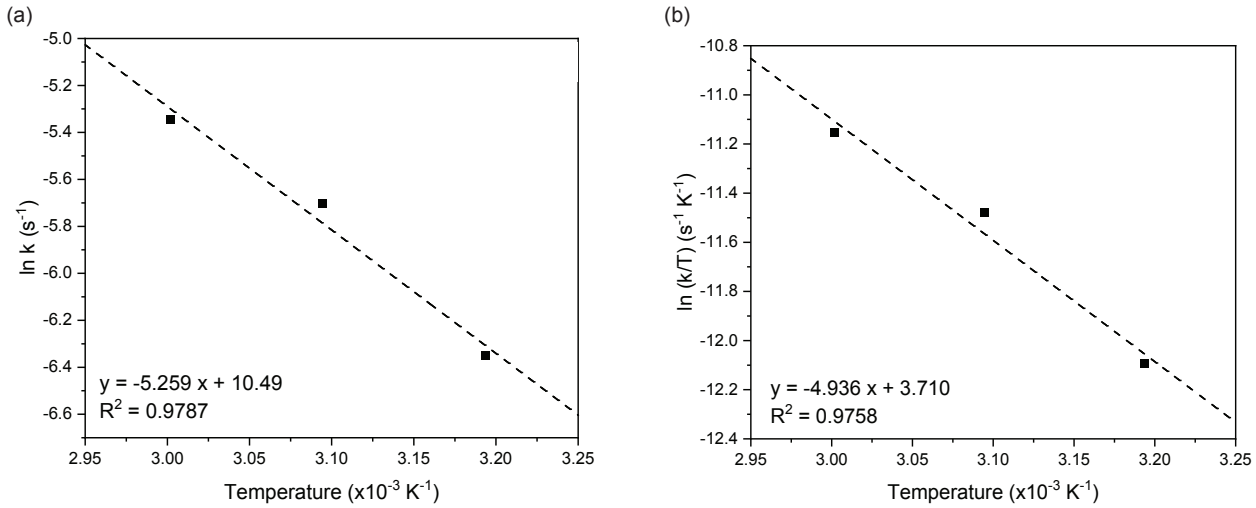

Figure 9. (a) Arrhenius plot; and (b) Eyring–Polanyi plot of temperature dependency in FFA esterification using Fe_3O_4/PVA/PTSA catalyst.

TABLE 1. VALUES OF THERMODYNAMIC FACTORS FOR THE FFA ESTERIFICATION REACTIONS CATALYSED BY Fe_3O_4/PVA/PTSA CATALYST

Standard enthalpy, ΔH° (kJ/mol)	Entropy of activation, ΔS° (kJ/mol)	Gibbs free energy, ΔG° (kJ/mol)			Coefficient of determination, R^2
		313.15 K	323.15 K	333.15 K	
41.04	-0.167	93.24	94.91	96.57	0.9758

CONCLUSION

In this study, sulphonic acids (BZSA, PTSA and SSA) and their DES counterparts (formed with PCM at a 3:1 molar ratio) were attempted to be supported on Fe_3O_4/PVA magnetic composites to yield heterogeneous SACs for the esterification of FFA in LPO. The screening results reveal that PTSA was compatible with the Fe_3O_4/PVA support material based on the catalytic activity in FFA esterification and that the pristine sulphonic acid components exhibited greater FFA conversion compared to the DES system. Subsequently, Fe_3O_4/PVA/PTSA was selected as the best performing catalyst for further optimisation in reaction conditions. At reaction conditions of 10 wt.% catalyst loading, 20:1 methanol-to-oil molar ratio, 5 hr of contact time and at 60°C, the LPO was pretreated to the FFA content value of 1.95%, corresponding to an FFA conversion of 79.81%. Additionally, the catalyst was recycled for five successive runs with fair stability and acceptable FFA conversion (>65%). The reaction kinetics revealed that the FFA esterification reaction using Fe_3O_4/PVA/PTSA follows the pseudo first order rate of reaction, requiring an activation energy of 43.72 kJ/mol. This study demonstrated the feasibility of certain sulphonic acids and DESs to be supported on the Fe_3O_4/PVA magnetic composite, with Fe_3O_4/PVA/PTSA being the viable catalyst choice for the pretreatment of low-quality oils through FFA esterification.

ACKNOWLEDGEMENT

The authors would like to acknowledge the grant provided by Universiti Malaya, RU Geran–Fakulti program – GPF015A-2023. The author Y. A. T. H. would like to extend their sincerest gratitude to Dr. Chan Mieow Kee and the Department of Chemical Engineering, SEGi University for providing assistance with laboratory facilities and equipment.

REFERENCES

Ali, R. M., Elkatory, M. R., & Hamad, H. A. (2020). Highly active and stable magnetically recyclable $CuFe_2O_4$ as a heterogenous catalyst for efficient conversion of waste frying oil to biodiesel. *Fuel*, *268*, 117297. https://doi.org/10.1016/j.fuel.2020.117297

Ali, S., Khan, S. A., Eastoe, J., Hussaini, S. R., Morsy, M. A., & Yamani, Z. H. (2018). Synthesis, characterization, and relaxometry studies of hydrophilic and hydrophobic superparamagnetic Fe_3O_4 nanoparticles for oil reservoir applications. *Colloids and Surfaces A: Physicochemical and Engineering Aspects*, *543*, 133–143. https://doi.org/10.1016/j.colsurfa.2018.02.002

American Oil Chemists Society (AOCS). (2017). *Official methods and recommended practices of the AOCS*.

Ba-Abbad, M. M., Benamour, A., Ewis, D., Mohammad, A. W., & Mahmoudi, E. (2022). Synthesis of Fe_3O_4 nanoparticles with different shapes through a co-precipitation method and their application. *JOM*, *74*(9), 3531–3539. https://doi.org/10.1007/s11837-022-05380-3

Bahadoran, A., Ramakrishna, S., Oryani, B., Al-Keridis, L. A., Nodeh, H. R., & Rezania, S. (2022). Biodiesel production from waste cooking oil using heterogeneous nanocatalyst-based magnetic polyaniline decorated with cobalt oxide. *Fuel*, *319*, 123858. https://doi.org/10.1016/j.fuel.2022.123858

Borton, J., Lopez, F. D. N., Doan, L., Holmes, W. E., & Benson, T. J. (2019). Conversion of high free fatty acid lipid feedstocks to biofuel using triazabicyclodecene catalyst (Homogeneous and heterogeneous). *Energy & Fuels*, *33*(4), 3322–3330. https://doi.org/10.1021/acs.energyfuels.9b00359

Cao, M., Peng, L., Xie, Q., Xing, K., Lu, M., & Ji, J. (2021). Sulfonated *Sargassum horneri* carbon as solid acid catalyst to produce biodiesel via esterification. *Bioresource Technology*, *324*, 124614. https://doi.org/10.1016/j.biortech.2020.124614

Chen, C., Wang, F., Li, Q., Wang, Y., & Ma, J. (2022). Embedding of SO_3H-functionalized ionic liquids in mesoporous MIL-101(Cr) through polyoxometalate bridging: A robust heterogeneous catalyst for biodiesel production. *Colloids and Surfaces A: Physicochemical and Engineering Aspects*, *648*, 129432. https://doi.org/10.1016/j.colsurfa.2022.129432

Chen, L., He, L., Zheng, B., Wei, G., Li, H., Zhang, H., & Yang, S. (2023). Bifunctional acid-activated montmorillonite catalyzed biodiesel production from non-food oil: Characterization, optimization, kinetic and thermodynamic studies. *Fuel Processing Technology*, *250*, 107903. https://doi.org/10.1016/j.fuproc.2023.107903

Fazelinia, F., Bayat, M., Nasri, S., Kamalzare, M., & Maleki, A. (2023). Chitosan@Tannic acid-supported Fe_3O_4 magnetic bionanocomposite as green and recyclable catalyst for the synthesis of Benzo[g]thiazolo[3,2-a] quinolones based on nitroketene N,S-Acetal. *Catalysis Surveys From Asia*, *27*(4), 391–405. https://doi.org/10.1007/s10563-023-09406-x

Gardy, J., Osatiashtiani, A., Céspedes, O., Hassanpour, A., Lai, X., Lee, A. F., Wilson, K., & Rehan, M. (2018). A magnetically separable SO_4/Fe-Al-TiO_2 solid acid catalyst for biodiesel production from waste cooking oil. *Applied Catalysis B: Environment and Energy*, *234*, 268–278. https://doi.org/10.1016/j.apcatb.2018.04.046

Ghorbani-Choghamarani, A., Taherinia, Z., & Tyula, Y. A. (2022). Efficient biodiesel production from oleic and palmitic acid using a novel molybdenum metal-organic framework as efficient and reusable catalyst. *Scientific Reports*, *12*(1), 10338. https://doi.org/10.1038/s41598-022-14341-4

Hayyan, A., Alam, M. Z., Mirghani, M. E., Kabbashi, N. A., Hakimi, N. I. N. M., Siran, Y. M., & Tahiruddin, S. (2010). Sludge palm oil as a renewable raw material for biodiesel production by two-step processes. *Bioresource Technology*, *101*(20), 7804–7811. https://doi.org/10.1016/j.biortech.2010.05.045

Hayyan, A., Qing, F. L. W., Salleh, M. Z. M., Basirun, W. J., Hamid, M. D., Saleh, J., Aljohani, A. S., Alhumaydhi, F. A., Zulkifli, M., Abdulmonem, W. A., Yeow, A. T., Nor, M. R. M., Hashim, M. A., & Al-Sabahi, J. N. (2023). Encapsulated paracetamol-based eutectic solvents for the treatment of low-grade palm oil mixed with microalgae oil. *Industrial Crops and Products*, *195*, 116322. https://doi.org/10.1016/j.indcrop.2023.116322

He, L., Chen, L., Zheng, B., Zhou, H., Wang, H., Li, H., Zhang, H., Xu, C. C., & Yang, S. (2023). Deep eutectic solvents for catalytic biodiesel production from liquid biomass and upgrading of solid biomass into 5-hydroxymethylfurfural. *Green Chemistry*, *25*(19), 7410–7440. https://doi.org/10.1039/d3gc02816j

Ibrahim, N. A., Rashid, U., Choong, T. S. Y., & Nehdi, I. A. (2020). Synthesis of nanomagnetic sulphonated impregnated Ni/Mn/Na_2SiO_3 as catalyst for esterification of palm fatty acid distillate. *RSC Advances*, *10*(10), 6098–6108. https://doi.org/10.1039/c9ra08115a

Kamalzare, M., Ahghari, M. R., Bayat, M., & Maleki, A. (2021). Fe_3O_4@chitosan-tannic acid bionanocomposite as a novel nanocatalyst for the synthesis of pyranopyrazoles. *Scientific Reports*, *11*(1), 20021. https://doi.org/10.1038/s41598-021-99121-2

Khan, Z., Javed, F., Shamair, Z., Hafeez, A., Fazal, T., Aslam, A., Zimmerman, W. B., & Rehman, F. (2021). Current developments in esterification

reaction: A review on process and parameters. *Journal of Industrial and Engineering Chemistry*, *103*, 80–101. https://doi.org/10.1016/j.jiec.2021.07.018

Krishnan, S. G., Pua, F., & Zhang, F. (2021). A review of magnetic solid catalyst development for sustainable biodiesel production. *Biomass and Bioenergy*, *149*, 106099. https://doi.org/10.1016/j.biombioe.2021.106099

Kurchania, R., Sawant, S. S., & Ball, R. J. (2014). Synthesis and characterization of magnetite/polyvinyl alcohol core-shell composite nanoparticles. *Journal of the American Ceramic Society*, *97*(10), 3208–3215. https://doi.org/10.1111/jace.13108

Lieu, T., Yusup, S., & Moniruzzaman, M. (2016). Kinetic study on microwave-assisted esterification of free fatty acids derived from *Ceiba pentandra* seed oil. *Bioresource Technology*, *211*, 248–256. https://doi.org/10.1016/j.biortech.2016.03.105

Liu, W., Wang, F., Meng, P., & Zang, S. (2020). Sulfonic acids supported on UIO-66 as heterogeneous catalysts for the esterification of fatty acids for biodiesel production. *Catalysts*, *10*(11), 1271. https://doi.org/10.3390/catal10111271

Lou, J., Babadi, M. R., Otadi, M., Tarahomi, M., Van Le, Q., Khonakdar, H. A., & Li, C. (2023). Agricultural waste valorization towards (nano) catalysts for the production of chemicals and materials. *Fuel*, *351*, 128935. https://doi.org/10.1016/j.fuel.2023.128935

Luo, N., Yang, Z., Tang, F., Wang, D., Feng, M., Liao, X., & Yang, X. (2019). Fe_3O_4/Carbon NanoDot hybrid nanoparticles for the indirect colorimetric detection of glutathione. *ACS Applied Nano Materials*, *2*(6), 3951–3959. https://doi.org/10.1021/acsanm.9b00854

Maleki, A., Niksefat, M., Rahimi, J., & Hajizadeh, Z. (2019). Design and preparation of Fe_3O_4@PVA polymeric magnetic nanocomposite film and surface coating by sulfonic acid via *in situ* methods and evaluation of its catalytic performance in the synthesis of dihydropyrimidines. *BMC Chemistry*, *13*(1), 19. https://doi.org/10.1186/s13065-019-0538-2

Maleki, B., Talesh, S. A., & Mansouri, M. (2022). Comparison of catalysts types performance in the generation of sustainable biodiesel via transesterification of various oil sources: A review study. *Materials Today Sustainability*, *18*, 100157. https://doi.org/10.1016/j.mtsust.2022.100157

Mandari, V., & Devarai, S. K. (2022). Biodiesel production using homogeneous, heterogeneous, and enzyme catalysts via transesterification and esterification reactions: A critical review. *BioEnergy Research*, *15*(2), 935–961. https://doi.org/10.1007/s12155-021-10333-w

Mok, C. F., Ching, Y. C., Osman, N. A. A., Muhamad, F., Junaidi, M. U. M., & Choo, J. H. (2020). Preparation and characterization study on maleic acid cross-linked poly(vinyl alcohol)/chitin/nanocellulose composites. *Journal of Applied Polymer Science*, *137*(35), 49044. https://doi.org/10.1002/app.49044

Olagbende, O. H., Falowo, O. A., Latinwo, L. M., & Betiku, E. (2021). Esterification of Khaya senegalensis seed oil with a solid heterogeneous acid catalyst: Modeling, optimization, kinetic and thermodynamic studies. *Cleaner Engineering and Technology*, *4*, 100200. https://doi.org/10.1016/j.clet.2021.100200

Perez, G. A. P., & Dumont, M. (2021). Polyvinyl sulfonated catalyst and the effect of sulfonic sites on the dehydration of carbohydrates. *Chemical Engineering Journal*, *419*, 129573. https://doi.org/10.1016/j.cej.2021.129573

Picciolini, E., Pastore, G., Del Giacco, T., Ciancaleoni, G., Tiecco, M., & Germani, R. (2023). Aquo-DESs: Water-based binary natural deep eutectic solvents. *Journal of Molecular Liquids*, *383*, 122057. https://doi.org/10.1016/j.molliq.2023.122057

Racar, M., Jerbić, I. Š., Glasovac, Z., & Jukić, A. (2023). Guanidine catalysts for biodiesel production: Activity, process modelling and optimization. *Renewable Energy*, *202*, 1046–1053. https://doi.org/10.1016/j.renene.2022.11.044

Rahimi, J., Niksefat, M., & Maleki, A. (2020a). Fabrication of Fe_3O_4@PVA-CU nanocomposite and its application for facile and selective oxidation of alcohols. *Frontiers in Chemistry*, *8*. https://doi.org/10.3389/fchem.2020.00615

Rahimi, J., Taheri-Ledari, R., Niksefat, M., & Maleki, A. (2020b). Enhanced reduction of nitrobenzene derivatives: Effective strategy executed by Fe_3O_4/PVA-10%Ag as a versatile hybrid nanocatalyst. *Catalysis Communications*, *134*, 105850. https://doi.org/10.1016/j.catcom.2019.105850

Rokhum, S. L., Changmai, B., Kress, T., & Wheatley, A. E. (2022). A one-pot route to tunable sugar-derived sulfonated carbon catalysts for

sustainable production of biodiesel by fatty acid esterification. *Renewable Energy*, *184*, 908–919. https://doi.org/10.1016/j.renene.2021.12.001

Roslan, N. A., Abidin, S. Z., Abdullah, N., Osazuwa, O. U., Rasid, R. A., & Yunus, N. M. (2022). Esterification reaction of free fatty acid in used cooking oil using sulfonated hypercrosslinked exchange resin as catalyst. *Process Safety and Environmental Protection*, *180*, 414–424. https://doi.org/10.1016/j.cherd.2021.10.020

Swami, P., Rathod, S., Choudhari, P., Patil, D., Patravale, A., Nalwar, Y., Sankpal, S., & Hangirgekar, S. (2023). Fe_3O_4@SiO_2@TDI@DES: A novel magnetically separable catalyst for the synthesis of oxindoles. *Journal of Molecular Structure*, *1292*, 136079. https://doi.org/10.1016/j.molstruc.2023.136079

Tang, Z., Lim, S., Pang, Y., Shuit, S., & Ong, H. (2020). Utilisation of biomass wastes based activated carbon supported heterogeneous acid catalyst for biodiesel production. *Renewable Energy*, *158*, 91–102. https://doi.org/10.1016/j.renene.2020.05.119

Tropecêlo, A. I., Caetano, C. S., Caiado, M., & Castanheiro, J. E. (2016). Biodiesel production from waste cooking oil over sulfonated catalysts. *Energy Sources Part A: Recovery Utilization and Environmental Effects*, *38*(2), 174–182. https://doi.org/10.1080/15567036.2012.747035

Wang, H., Zhou, H., Yan, Q., Wu, X., & Zhang, H. (2023). Superparamagnetic nanospheres with efficient bifunctional acidic sites enable sustainable production of biodiesel from budget non-edible oils. *Energy Conversion and Management*, *297*, 117758. https://doi.org/10.1016/j.enconman.2023.117758

Wang, R., Qin, H., Song, Z., Cheng, H., Chen, L., & Qi, Z. (2022). Toward reactive extraction processes for synthesizing long-chain esters: A general approach by tuning bifunctional deep eutectic solvent. *Chemical Engineering Journal*, *445*, 136664. https://doi.org/10.1016/j.cej.2022.136664

Wang, Y., Meng, X., Tian, Y., Kim, K. H., Jia, L., Pu, Y., Leem, G., Kumar, D., Eudes, A., Ragauskas, A. J., & Yoo, C. G. (2021). Engineered sorghum bagasse enables a sustainable biorefinery with p-hydroxybenzoic acid-based deep eutectic solvent. *ChemSusChem*, *14*(23), 5235–5244. https://doi.org/10.1002/cssc.202101492

Wang, Y., Wang, D., Tan, M., Jiang, B., Zheng, J., Tsubaki, N., & Wu, M. (2015). Monodispersed hollow SO_3H-functionalized carbon/silica as efficient solid acid catalyst for esterification of oleic acid. *ACS Applied Materials & Interfaces*, *7*(48), 26767–26775. https://doi.org/10.1021/acsami.5b08797

Wang, Y., Yang, X., Xu, J., Wang, H., Wang, Z., Zhang, L., Wang, S., & Liang, J. (2019). Biodiesel production from esterification of oleic acid by a sulfonated magnetic solid acid catalyst. *Renewable Energy*, *139*, 688–695. https://doi.org/10.1016/j.renene.2019.02.111

Xie, W., & Li, J. (2023). Magnetic solid catalysts for sustainable and cleaner biodiesel production: A comprehensive review. *Renewable and Sustainable Energy Reviews*, *171*, 113017. https://doi.org/10.1016/j.rser.2022.113017

Xie, W., & Wang, H. (2020). Immobilized polymeric sulfonated ionic liquid on core-shell structured Fe_3O_4/SiO_2 composites: A magnetically recyclable catalyst for simultaneous transesterification and esterifications of low-cost oils to biodiesel. *Renewable Energy*, *145*, 1709–1719. https://doi.org/10.1016/j.renene.2019.07.092

Yu, J., Wang, Y., Sun, L., Xu, Z., Du, Y., Sun, H., Li, W., Luo, S., Ma, C., & Liu, S. (2021). Catalysis preparation of biodiesel from waste schisandra chinensis seed oil with the ionic liquid immobilized in a magnetic catalyst: Fe_3O_4@SiO_2@[C4mim]HSO_4. *ACS Omega*, *6*(11), 7896–7909. https://doi.org/10.1021/acsomega.1c00504

Yusuf, B. O., Oladepo, S. A., & Ganiyu, S. A. (2023). Biodiesel production from waste cooking oil via β-zeolite-supported sulfated metal oxide catalyst systems. *ACS Omega*, *8*(26), 23720–23732. https://doi.org/10.1021/acsomega.3c01892

Zhang, H., Gao, J., Zhao, Z., Chen, G. Z., Wu, T., & He, F. (2016). Esterification of fatty acids from waste cooking oil to biodiesel over a sulfonated resin/PVA composite. *Catalysis Science & Technology*, *6*(14), 5590–5598. https://doi.org/10.1039/c5cy02133b

Zhang, Q., Lei, Y., Li, L., Lei, J., Hu, M., Deng, T., Zhang, Y., & Ma, P. (2023). Construction of the novel PMA@Bi-MOF catalyst for effective fatty acid esterification. *Sustainable Chemistry and Pharmacy*, *33*, 101038. https://doi.org/10.1016/j.scp.2023.101038

Zhang, Q., Luo, Q., Wu, Y., Yu, R., Cheng, J., & Zhang, Y. (2021). Construction of a Keggin heteropolyacid/Ni-MOF catalyst for esterification of fatty acids. *RSC Advances*, *11*(53), 33416–33424. https://doi.org/10.1039/d1ra06023f

Zheng, B., Chen, L., He, L., Wang, H., Li, H., Zhang, H., & Yang, S. (2024). Facile synthesis of chitosan-derived sulfonated solid acid catalysts for realizing highly effective production of biodiesel. *Industrial Crops and Products*, *210*, 118058. https://doi.org/10.1016/j.indcrop.2024.118058

Zhong, Y., Zhang, P., Zhu, X., Li, H., Deng, Q., Wang, J., Zeng, Z., Zou, J., & Deng, S. (2019). Highly efficient alkylation using hydrophobic sulfonic acid-functionalized biochar as a catalyst for synthesis of high-density biofuels. *ACS Sustainable Chemistry & Engineering*, *7*(17), 14973–14981. https://doi.org/10.1021/acssuschemeng.9b03190

Zhou, R., Ye, B., & Hou, Z. (2023). Synthesis of acetylglycerols over hierarchical porous sulfonated polymeric solid acid. *Fuel*, *354*, 129325. https://doi.org/10.1016/j.fuel.2023.129325